Available online at www.sciencedirect.com
SCIENCE DIRECT®
Thermochimica Acta 401 (2003) 27–41
thermochimica acta
www.elsevier.com/locate/tca

Thermal ageing of rocket propellant formulations containing ε-HNIW (ε-CL20) investigated by heat generation rate and mass loss☆

Manfred A. Bohn*

Fraunhofer-Institut für Chemische Technologie (ICT), Postfach 1240, D-76318 Pfinztal-Berghausen, Germany

Received 11 June 2002; received in revised form 14 October 2002; accepted 18 October 2002

Abstract

New types of rocket propellant batches have been formulated with the objective of achieving higher burning rates. The main ingredients are (1) the energetic plasticizers glycidyl azide polymer-α,ω-diazide (GAP)-A (short chain GAP with azide end groups), trimethylolethane trinitrate (TMETN) and 1,2,4-butanetriol trinitrate (BTTN), (2) the energetic substances ammonium perchlorate (AP) and ε-CL20 (ε-HNIW, hexanitrohexazaisowurtzitane, crystallised in ε-phase). The binder is GAP (glycidyl azide polymer, diol component) cured with the polyisocyanate Desmodur^{TM} N100. From the point of view of stability and ageing, the interesting fact is that the formulations contain none of the typical stabilisers for the nitric acid ester components TMETN and BTTN, although their contents range up to 21 mass%. One reason for doing so is to increase the content of the high energy ingredients. Seven formulations were examined in more detail. To assess basic stability the autoignition temperature test, Dutch mass loss test and vacuum stability test were used. To investigate ageing, two measurement quantities are applied: heat generation rate (heat flow) as function of time at 70, 80 and 89 °C and mass loss as function of time at the temperatures of 70, 80 and 90 °C. The evaluation of the measurements was done with reaction kinetic models. One batch (#189) containing BTTN shows significantly lower activation energy and pre-exponential factor. From mass loss one gets as activation energy for #189 of 101 kJ mol^{-1} in comparison to the range of 126–135 kJ mol^{-1} for the six other batches. But, based on the ageing caused by chemical decomposition reactions, all seven batches showed a good ageing behaviour. A use time period of up to 20 years of use seems realistic.

Keywords: Thermal ageing; Energetic material; Hexanitrohexazaisowurtzitane (HNIW); Heat generation rate; Mass loss; Kinetic model evaluation

1. Introduction

The objective of this investigation is to evaluate the types of ingredient mix named HFK as possible rocket propellants with acceptable ageing behaviour and to correlate it with their compositions, which are shown in Table 1 for seven HFK batches numbered from 178 to 189. The compositions are designed to get high burning rates. Information about the burning behaviour can be found in [1]. Using the data from typical stability tests, it is not possible to predict the ageing caused by decomposition reactions. The purpose of these tests is to get basic stability data in a short time, because the applied test temperatures of about

☆ Paper presented at the 3rd International Symposium on the Heat Flow Calorimetry of Energetic Materials, French Lick Springs, Indiana, USA, 8–10 April 2002.

* Tel.: +49-721-4640-162; fax: +49-721-4640-111.
E-mail address: manfred.bohn@ict.fhg.de (M.A. Bohn).

0040-6031/03/$ – see front matter © 2003 Published by Elsevier Science B.V.
doi:10.1016/S0040-6031(03)00052-2

100 °C and more are much higher than the meteorologically determined in-service temperatures, which are not higher than about 71 °C [2]. This is the possible maximum induced daily temperature in the material beneath its surface in hot and dry areas. To assess ageing one needs time-temperature data of the properties between 50 °C and a maximum of 90 °C. For unknown formulations simplified methods using reduced measurement data sets are not applicable due to the lack of the necessary data base. To establish such a data base, heat generation rates and mass losses as function of time and temperature have been determined. With unknown formulations at least two methods with a different probing of the material should be used. The two types of probing here are the split-off of decomposition gases and the heats of reactions. The summarised effect of the reaction heats was measured as heat generation rate using a microcalorimeter of type TAM (Thermal Activity Monitor), produced by Thermometric AB, Sweden. The split-off gases were determined as mass loss by weighing of samples stored in vials inserted in PID-controlled ovens, whereby the weighing intervals were adjusted to the decomposition rate.

Table 1 also lists the data for the heats of explosion Q_{EX} of the formulations. The values have been calculated using the ICT Thermodynamic Code and the data from the ICT Thermochemical Data Base [3]. Experimentally Q_{EX} is the heat produced by burning of the samples in a calorimetric bomb apparatus in an inert atmosphere. To determine the heat of combustion a pressurised oxygen atmosphere is used.

2. Results

2.1. Basic stability test data

Three tests have been applied: autoignition temperature test (AIT), Dutch mass loss test (Dutch stability test, DT), vacuum stability test (VST). Descriptions of the tests can be found in [4–6]. To determine the autoignition temperature (thermally induced deflagration) the dynamic method was used. The start temperature was 100 °C. The sample of 0.2 g is then heated up with 5 °C/min in glass vial with a Wood's metal bath. The temperature of reaction, with these batches always recognised as a bang, is recorded as autoignition temperature. The Dutch stability test is based on mass loss measurements. An amount of 4 g per glass vial is heated at 105 °C or 110 °C for 72 h, whereby during the first 8 h the vials are open to facilitate the escape of volatiles. Then the vials are weighed and heated further, closed with an inserted ground glass stopper. The mass loss between 8 and 72 h is used as criterion. The VST is well described in [6]. It determines the amount of split-off gases in an evacuated glass apparatus with a defined sample amount over a given time period at a given test temperature. The test

Table 1
Composition of the seven investigated HFK batches with the numbers 178–189 and their heats of explosion Q_{EX} with water as liquid and water as gaseous

	Batch #						
	178	180	181	182	184	185	189
GAP-A (mass%)	12.25	14	9	–	–	10.5	9
TMETN (mass%)	12.25	14	9	18	21	10.5	2.25
BTTN (mass%)	–	–	–	–	–	–	6.75
GAP-N100 (mass%)	10.5	7	12	12	14	14	12
ε-CL20 (mass%)	42	42	47	47	42	42	47
AP (mass%)	20	20	20	20	20	20	20
Others (mass%)	3	3	3	3	3	3	3
Q_{EX} (gaseous water) ($J\,g^{-1}$)	4540	4670	4700	5050	4880	4510	4750
Q_{EX} (liquid water) ($J\,g^{-1}$)	4840	4940	4960	5370	5200	4750	5020

TMETN: trimethylolethane trinitrate; BTTN: 1,2,4-butanetriol trinitrate; GAP: glycidyl azide polymer (polyurethane prepolymer, diol component); GAP-A: short chain GAP with N_3-end groups instead of OH-end groups; N100: Desmodur^{TM} N100 (Bayer AG, Germany), polyisocyanate (curing component); AP: ammonium perchlorate; ε-CL20: hexanitrohexazaisowurtzitane (HNIW) (2,4,6,8,10,12-hexanitro-2,4,6,8,10,12-hexaaza-tetracyclo [5.5.0.0^{5,9}.0^{3,11}]-dodecane), crystallised in ε-phase.

Table 2
Results of the stability tests

	Limit value	Batch #						
		178	180	181	182	184	185	189
Autoignition temperature, 0.2 g, 5 °C min^{-1} heat rate (°C)	≥170	172	173	175	172	170	176	177
Dutch ML test, 105 °C, 4 g, ML at 72 h minus ML at 8 h (%)	≤2	0.78	0.75	0.68	0.90	1.11	0.80	0.75
Vacuum stability, 100 °C, 40 h, 2.5 g (ml g^{-1})	≤1.2	1.55	1.56	1.32	1.74	2.06	1.49	1.54

conditions are given in Table 2. They vary corresponding to the type of materials. The results of the AIT and of the DT fulfil the corresponding limit criteria. The data of the VST are all above the limit value but this is caused by the high test temperature. With formulations containing nitric acid ester compounds a temperature of 90 °C is generally used, but here 100 °C was applied because of comparability with other data sets. According to the rule of thumb, the reduction of the temperature by 10 °C reduces the evolved gas amount by a factor of about 3 and the given limit of 1.2 ml g^{-1} is fulfilled. The actual factors found with these batches are listed in Table 7.

2.2. Mass loss data

As an example of all investigated HFK batches the mass loss data of HFK 178 at 90 °C are shown in Fig. 1 as function of time. The data of both parallel samples coincide, which was the case for all batches at all measurement temperatures. In Fig. 2 the averaged ML data at 90 °C of each of the seven HFK batches can be seen. HFK 184 with 21 mass% TMETN as the only plasticizer has the highest decomposition rate k_{ML} (means the greatest slope of the linear part of the curves), followed by HFK 189 with TMETN+BTTN and GAP-A as the system of plasticizers. This is followed by HFK 182 with 18 mass% TMETN. HFK 180 and 181 show the lowest decomposition rate. In Fig. 2 the curves obtained according to model 'ML: linear + exponential' are also included, see Section 3.1. All data descriptions are very good, which is also documented by the high correlation coefficients. The ML curves show an initial flexure, then a linear increase. In terms of reaction kinetics, the linear increase means a global decomposition reaction of zero order. In detail, the decomposition course is much more complex, and therefore this linear part of the mass loss is named decomposition

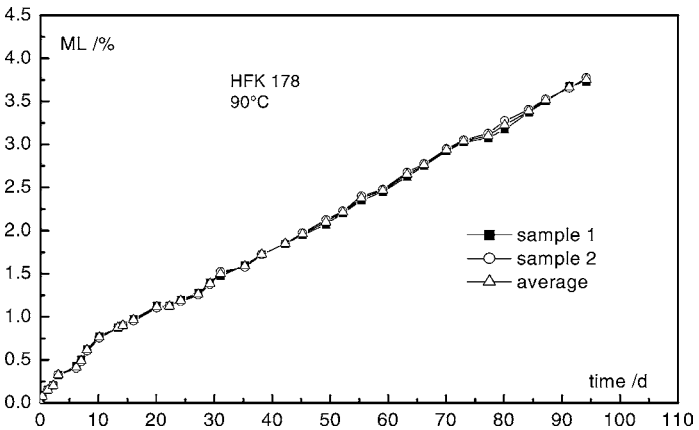

Fig. 1. Mass loss data of HFK 178 at 90 °C. The data of both parallel samples coincide.

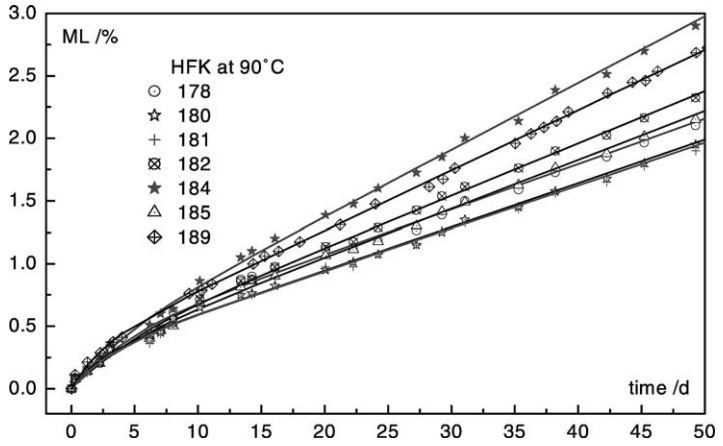

Fig. 2. Mass loss data of seven HFK batches at 90 °C. The lines are the model 'ML: linear + exponential'.

reaction of pseudo zero order. Figs. 3 and 4 show the averaged ML data and modelling at 80 °C and at 70 °C. Qualitatively the behaviour is identical to that found at 90 °C. But HFK 189 changes its ageing behaviour at lower temperature; it is now the batch with the highest mass loss rate.

2.3. Heat generation rate data

The heat generation rates (HGR) d*Q*/d*t* of the HFK batches at 89, 80 and 70 °C are shown in Figs. 5–7. With the used microcalorimeter 89 °C was the highest possible measurement temperature. By integration over time, the heat generations (HG) *Q* are obtained, which are also presented in the figures with bold lines, correlating with the right ordinates. The measurement procedure used is different compared with the one used for the mass loss measurements. In that case, new unstressed sample material was taken at each temperature. Here the measurements start with unstressed material at 80 °C, Fig. 6. Then, using the same samples, the measurements continued at 70 °C (Fig. 7) and then the measurements were taken at 89 °C (Fig. 5). This procedure is named 'pseudo-iso-conversion' method, also abbreviated to 'pic mode'. The conversion achieved at 80 °C is nearly not changed at 70 °C

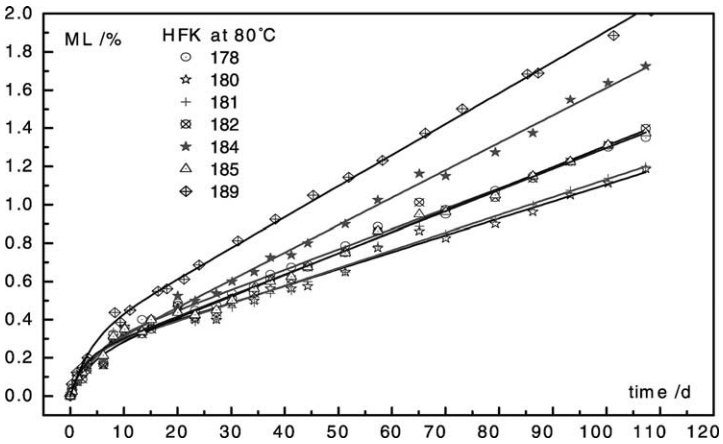

Fig. 3. Mass loss data of seven HFK batches at 80 °C. The lines are the model 'ML: linear + exponential'.

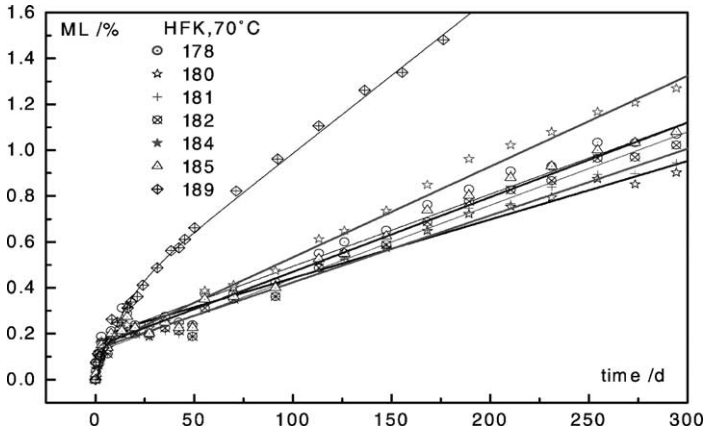

Fig. 4. Mass loss data of seven HFK batches at 70 °C. The lines are the model 'ML: linear + exponential'.

because of the lower decomposition rate and the short measurement times. At 89 °C one has again nearly the same conversion state as at 80 °C. At this state of conversion the Arrhenius parameters can be obtained in a much shorter time than using unstressed material at all measurement temperatures. This method works well if the sample decomposes with one defined reaction. In the case of a defined reaction of zero order this method is even free of error. One measures just the HGR, which is directly proportional to the reaction rate constant. With autocatalytic systems the HGR will not scale correctly in pic mode.

There is one obvious difference in the HGR curves measured using unstressed material and in pic mode. At the beginning, the unstressed material shows a peak in the curves. This is the HGR caused by the residual curing reaction of the polyurethane binder and from the initial decomposition reaction, which both does not occur in the pic mode measurements because of finishing these reactions at 80 °C. To separate the curing reaction from the main decomposition part

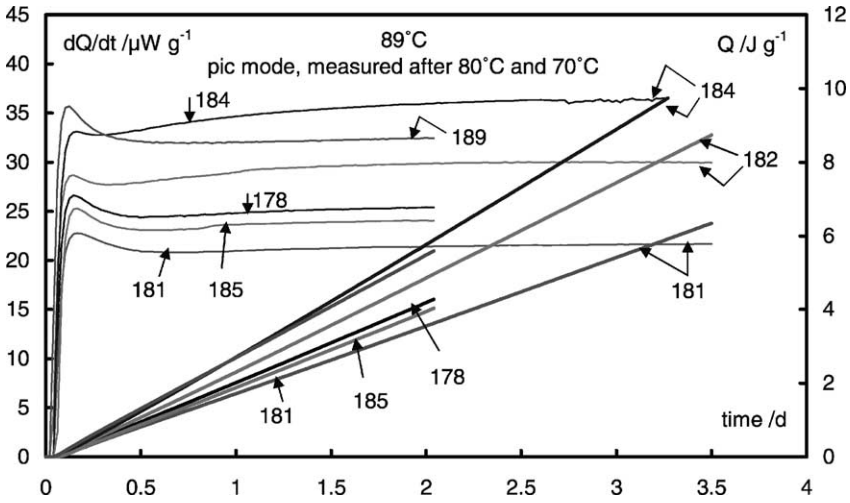

Fig. 5. Heat generation rate d*Q*/d*t* and heat generation *Q* (bold lines) of HFK batches at 89 °C, determined in pseudo-iso-conversion mode after measurements had been taken at 80 and 70 °C.

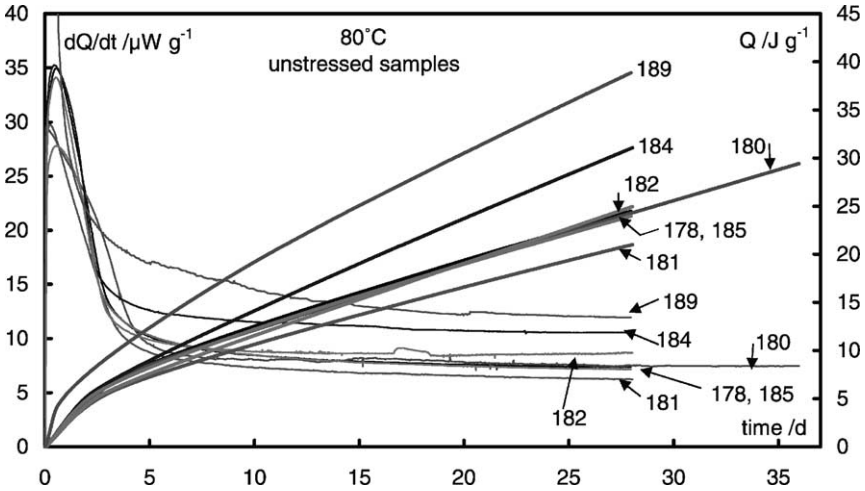

Fig. 6. Heat generation rate dQ/dt and heat generation Q (bold lines) of HFK batches at 80 °C, determined using unstressed samples.

(pseudo zero order reaction) relatively long measurement times have been necessary, even at 80 °C. From Fig. 6 one can assume that the curing reaction is nearly immeasurable after about 15 days. The curing reaction overlays the initial decomposition reaction found with mass loss measurements, see Section 3.2.

For all HFK batches the HG has an analogous course to the ML: the initial flexure (with unstressed material) is followed by a linear increase, which again is indicative of a global decomposition reaction of pseudo zero order. Both measurement quantities mass loss and heat generation rate lead to the same interpretation of the data. However, the residual curing as an addition reaction to form the polyurethane binder is not recognised by mass loss, but this is an advantage of this method in the context of stability and ageing assessment. In Table 3 HGR data are compiled. All data are taken in the region with a pseudo zero order behaviour, that means the HGR is nearly constant with time. Additionally the extrapolated HGR

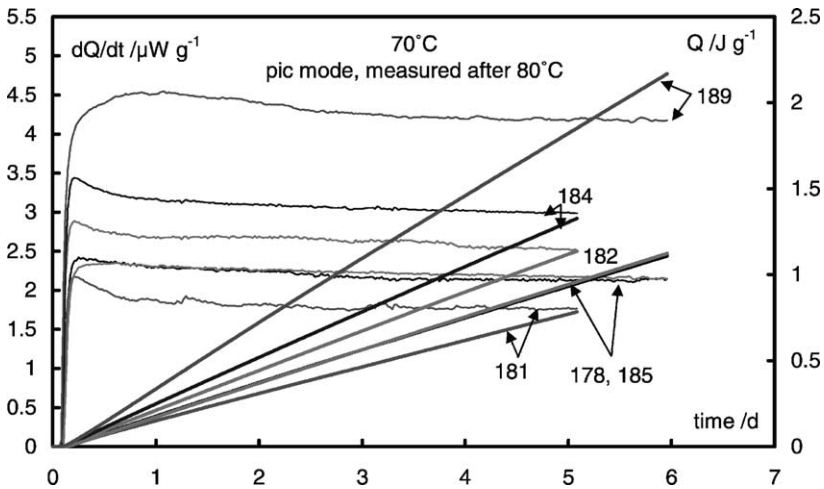

Fig. 7. Heat generation rate dQ/dt and heat generation Q (bold lines) of HFK batches at 70 °C, determined in pseudo-iso-conversion mode after measurements had been taken at 80 °C.

Table 3
Heat generation rate data dQ/dt ($\mu W\,g^{-1}$) from the linear part in HG of HFK batches obtained after the given measurement times

	Time (day)	178	180	181	182	184	185	189
70 °C, pic mode after 80 °C	3.0	2.16	–	1.76	2.62	3.04	2.22	4.25
80 °C unstressed sample material	27.5	7.38	7.46	6.26	8.69	10.55	7.16	11.95
89 °C, pic mode after 80, 70 °C	2.0	25.43	–	21.42	29.87	35.95	24.08	32.48
90 °C, extrapolated from 80 and 89 °C[a]	–	29.18	–	24.56	34.26	41.20	27.55	36.30

'pic' mode means measured in 'pseudo-iso-conversion' mode. Included are the extrapolated data for 90 °C.
[a] Equation used for extrapolation: $\dot{q}(90\,^{\circ}C) = \dot{q}(80\,^{\circ}C)(\dot{q}(89\,^{\circ}C)/\dot{q}(80\,^{\circ}C))^{1019}$.

at 90 °C are listed. They have been obtained with the formula given in Table 3. The extrapolation is based on the Arrhenius dependence.

3. Discussion

3.1. Mass loss

The mass loss data are analysed using the model 'ML: linear + exponential', corresponding to 'zero order reaction + first order reaction'. The reaction scheme is shown in Eq. (1), it is formulated in molar concentrations with $(-\Delta H_{R,i})$ as reaction enthalpies.

$$\begin{aligned} \mathrm{A} &\xrightarrow{k_\mathrm{A}} \mathrm{C} + \mathrm{S} \quad (-\Delta H_{R,\mathrm{A}}) \\ \mathrm{V} &\xrightarrow{k_\mathrm{V}} \mathrm{V}_{-} \quad (-\Delta H_{R,\mathrm{V}}) \end{aligned} \tag{1}$$

The global main component A of a formulation decomposes to gaseous products C (in the scheme C corresponds to all gaseous products) and in the residue remaining products S (S corresponds to all remaining products). On the possible products C, S and V only general statements are possible. Gaseous species can be N_2, N_2O, CO, CO_2, HCN, H_2O, NO, NO_2, which have been detected during thermal decomposition of CL20. Solid residues may be condensed oligomeric substances from CL20 and from GAP. The main component A is assigned to a reaction of zero order. The minor component V can evaporate or decompose into gaseous products V_- according to a reaction of first order. The initial mass of V in the sample is expressed as part of the total sample mass M, $M_\mathrm{V}(0) = aM(0)$. The detailed derivation can be found in the literature [7,8]. Using the following model settings, Eq. (2) results, formulated for the mass loss ML.

- $M_\mathrm{S}(0)$ is zero.
- The mass M_N of a non-reacting ingredient is small.
- The molar mass ratio $m_\mathrm{C}/m_\mathrm{A}$ is set approximately to one.

$$\mathrm{ML}(t,T) = \mathrm{OF}_\mathrm{ML} + 100\% \left(\frac{m_\mathrm{C}}{m_\mathrm{A}} (1-a) k_\mathrm{ML}(T) t + a(1 - \exp(-k_\mathrm{V}(T)t)) \right) \tag{2}$$

$$k_\mathrm{ML}(T) = k_\mathrm{A}(T) \frac{m_\mathrm{A}}{M_\mathrm{A}(0)} \tag{3}$$

$k_\mathrm{ML}(T)$ is connected with the reaction rate constant $k_\mathrm{A}(T)$ from Eq. (1) via Eq. (3). In the experimental data the offset OF_ML was always zero. Then only three model parameters remain to be determined: a, k_V and k_ML, which is done with a non-linear fit algorithm.

The model results are summarised in Table 4. The reaction rate constant k_ML and the mass fraction a are scaled by 100%. The correlation coefficients of the model descriptions of the seven batches are high at all temperatures. Qualitatively, all HFK batches show identical ageing behaviour (see Figs. 2–4). The Arrhenius parameters of $k_\mathrm{ML}(T)$ 100% are given in Table 5. Also a step by step evaluation was performed, that means the calculation of the Arrhenius parameters using pairs of temperatures. From this, one can see the tendency that the activation energies decrease with decreasing temperatures. The changes in Ea are always greater than the standard deviations. In Fig. 8 the corresponding Arrhenius plots are given. This effect is pronounced with HFK 189, the lower value of 86.3 kJ mol^{-1} is about 26% less than the higher value. The values for a and $k_\mathrm{V}(T)$ seem to contain several contributions: evaporation of water and maybe some other volatiles and decomposition of ingredients. This

Table 4
The model parameters k_{ML}, k_V and a, and the correlation coefficients of the model fits

	178	180	181	182	184	185	189
90 °C							
k_{ML} × 100% (% per day)	0.036	0.035	0.034	0.042	0.054	0.039	0.048
k_V (per day)	0.24	0.41	0.34	0.22	0.24	0.25	0.43
a × 100% (%)	0.35	0.25	0.26	0.29	0.31	0.27	0.30
Correlation coefficient	0.9995	0.9996	0.9995	0.9993	0.9993	0.9996	0.9997
80 °C							
k_{ML} × 100 (% per day)	0.0106	0.0089	0.0093	0.0114	0.0145	0.0111	0.0160
k_V (per day)	0.244	0.297	0.352	0.275	0.322	0.419	0.23
a × 100% (%)	0.24	0.22	0.21	0.18	0.17	0.19	0.30
Correlation coefficient	0.997	0.995	0.996	0.997	0.999	0.999	0.9994
70 °C							
k_{ML} × 100% (% per day)	0.00315	0.00255	0.00291	0.0032	0.00395	0.00325	0.00679
k_V (per day)	0.656	0.396	0.558	0.719	0.415	0.542	0.080
a × 100% (%)	0.18	0.19	0.14	0.12	0.14	0.15	0.31
Correlation coefficient	0.995	0.994	0.996	0.997	0.997	0.997	0.999

k_{ML} and a are scaled by 100%.

explains the inverse increase of the values of most of $k_V(T)$.

To assess the in-service time periods one defines an allowed limit value of a quantity. With mass loss generally 3% is taken. The degree of mass change is $y_{MŁ}$ and given by Eq. (4). With Eq. (5) the times $ty_{MŁ,L}(T)$ to reach the given limit value M_L or the limit degree $y_{MŁ,L}$ can be calculated. As mass loss the quantity $y_{ML} = (1-y_{MŁ})$ is a conversion quantity. The times to reach 3% ML at 50 °C are listed in Table 6.

$$y_{MŁ,L} = \frac{M_L}{M(0)} = M_{r,L} = 1 - k_{ML}(T)\, ty_{MŁ,L}(T) \quad (4)$$

$$ty_{MŁ,L}(T) = \frac{1 - y_{MŁ,L}}{k_{ML}(T)} = \frac{y_{ML,L}}{k_{ML}(T)} = ty_{ML,L}(T) \quad (5)$$

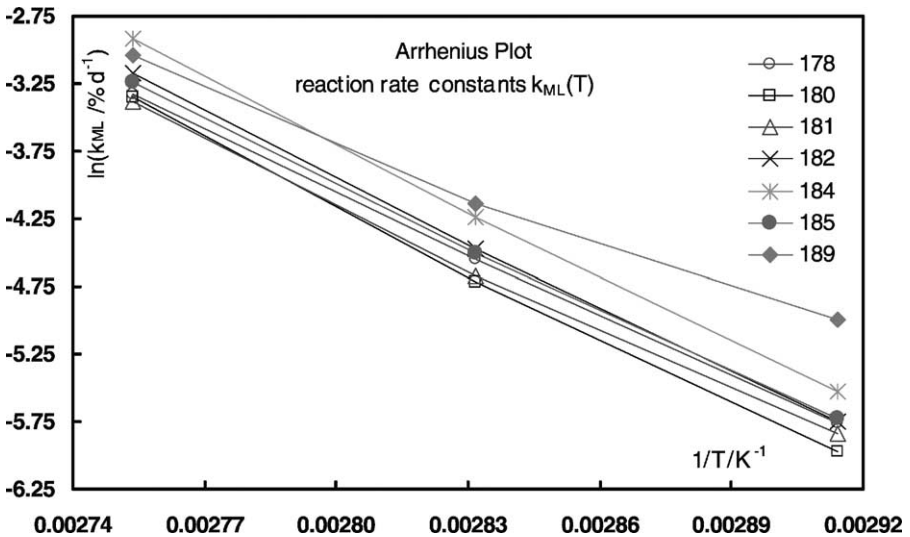

Fig. 8. Arrhenius plot of the reaction rate constants $k_{ML}(T)$ from mass loss measurements. The tendency of decreasing activation energy with decreasing temperature is indicated. The reversal in the reactivity between HFK 189 and 184 can be seen.

Table 5
Arrhenius parameters of the reaction rate constants $k_{ML}(T) \times 100\%$

Temperature range (°C)		178	180	181	182	184	185	189
90–70	Ea_{ML} (kJ mol^{-1})	126.2 ± 2.3	135.6 ± 5.8	127.2 ± 6.1	133.3 ± 3.2	135.4 ± 2.7	128.7 ± 3.0	101.1 ± 8.9
	$\log(Z_{ML}$ (% per day))	16.70 ± 0.35	18.03 ± 0.86	16.82 ± 0.90	17.79 ± 0.47	18.20 ± 0.40	17.09 ± 0.40	13.21 ± 1.32
	Correlation coefficient	0.9998	0.9991	0.9989	0.9997	0.9998	0.9997	0.9962
		Pairs of temperature evaluation						
90–80	Ea_{ML} (kJ mol^{-1})	130.4	146.0	138.2	139.1	140.2	134.0	117.1
	$\log(Z_{ML}$ (% per day))	17.31	19.55	18.41	18.62	18.90	17.86	15.53
80–70	Ea_{ML} (kJ mol^{-1})	122.3	125.9	117.1	128.0	130.9	123.7	86.3
	$\log(Z_{ML}$ (% per day))	16.11	16.58	15.28	16.99	17.53	16.34	10.97

A calculation of the parameters using pairs of temperatures is shown, indicating the tendency of the change in the parameters going from higher to lower temperatures. The change in activation energy with temperature is greater than the standard deviations.

Table 6
Times $ty_{ML,L}(T)$ in years to reach a mass loss of 3% at 50 °C, calculated according to Eq. (5) with the corresponding Arrhenius parameters for $k_{ML}(T)$, in dependence of the temperature range

Temperature range (°C)		178	180	181	182	184	185	189
90–70	$ty_{ML,L}$ (50 °C)/a	41.1	63.6	45.2	46.9	39.9	42.5	11.1
90–80	$ty_{ML,L}$ (50 °C)/a	48.2	92.1	69.7	60.1	47.5	51.8	20.6
80–70	$ty_{ML,L}$ (50 °C)/a	37.5	48.5	36.6	41.2	35.0	37.1	7.8

The often referred factors for an increase or decrease of the reaction rate constants in changing the temperature by 10 °C are given in Table 7; the experimental ones and the ones calculated with the corresponding activation energies.

3.2. Heat generation rate

The two parts of the model for mass loss, Eq. (2), are given with heat generation by Eq. (6) for the pseudo zero order reaction and by Eq. (7) for the first order part. OF_Q is as OF_{ML} a possible offset. A third contribution to the total HG is shown by Eq. (8). It stands for the residual curing reaction of the binder. This curing reaction is no longer present in the materials measured in pic mode as is true also for the first order reaction part.

$$Q_A(t,T) = OF_Q + (k_{Q,A}(T)t) \quad \text{with}$$
$$k_{Q,A}(T) = k_A(T)(-\Delta H_{R,A}) \tag{6}$$

$$Q_V(t,T) = OF_Q + (-\Delta H_{R,V})a(1 - \exp(-k_V(T)t)) \tag{7}$$

$$Q_{curing}(t,T) = OF_Q + (-\Delta H_{R,curing})F_{curing}(t,T) \tag{8}$$

For the kinetic expression $F_{curing}(t, T)$ a simple approximation would be a bimolecular addition reaction between the OH-groups of GAP and the isocyanate groups of N100. Some diffusion determined part in this reaction would be neglected. The complete model has then many parameters to be fitted. Including the heats of reaction one has from Eq. (6) two parameters, from Eq. (7) three and from Eq. (8) also at least three. The shape of the HGR curves is to un-structured to get any significant data by fitting eight parameters. Even with information about $(-\Delta H_{R,curing})$, and using data from mass loss for k_V and for a, to much parameters remain. Therefore, a full modelling was not obtainable and the nearly constant heat generation rates (representing formal zero order reactions) have been used for the evaluation.

In Table 8 the Arrhenius parameters determined using the experimental data from Table 3 are presented. As a reminder, index G indicates the global type of the heat generation rates measured in complex systems such as the HFK batches. Also an evaluation was made using pairs of temperatures. The same results are obtained here as were obtained with mass loss. As the temperature decreases, the tendency of decreasing activation energies is recognisable. Fig. 9 shows the corresponding Arrhenius plots. The factors for increase or decrease of the reaction rate constants in heat generation with a 10 °C temperature step are listed. They show qualitatively the same behaviour as the factors for mass loss rates.

The in-service time periods based on HGR and HG, respectively can be determined analogously to the same way as with mass loss [9]. One uses always a conversion quantity. The times to reach the limit value of a conversion are the looked for use time periods. But there is one essential difference. For mass loss the easily determinable initial value $M(0)$ is available as the reference. For HG the corresponding reference value is the value obtained after the complete decomposition reaction of the substance, *but at the temperatures of interest*. These data are practically not obtainable on formulations investigated here. It would take many years of measurement. Therefore the heat of explosion Q_{EX} is taken as $Q_{reference}$. This may result in a systematic error, because the decomposition reactions are different when obtaining Q_{EX} compared with the slow ageing at temperatures between 30 and 90 °C. In the first case thermodynamics nearly completely controls the reaction channels, in the second case kinetic control is dominant. Eq. (9) gives the definition of the degree of energy change in the

Table 7
Factors for increase/decrease of the reaction rate constant in mass loss with a 10 °C temperature step, determined according to the experimental data and calculated with the derived activation energies (from 70 to 90 °C)

Temperature range (°C)	178		180		181		182		184		185		189	
	Experimental	Ea	Experimental	Ea	Experimental	Ea	Experimental	Ea	Experimental	Ea	Experimental	Ea	Experimental	Ea
90–100		3.06		3.33		3.09		3.27		3.33		3.13		2.45
80–90	3.40	3.26	3.93	3.57	3.66	3.30	3.68	3.49	3.72	3.56	3.51	3.34	3.00	2.58
70–80	3.37	3.50	3.49	3.84	3.20	3.54	3.56	3.76	3.67	3.83	3.41	3.59	2.36	2.73
60–70		3.77		4.16		3.81		4.07		4.16		3.87		2.90

Table 8
Arrhenius parameters calculated from the pseudo zero order HGR data given in Table 3

Temperature range (°C)		178	180	181	182	184	185	189
89–70	$Ea_{Q,G}$ (kJ mol^{-1})	134.8 ± 5.9	–	135.4 ± 5.2	134.2 ± 6.1	135.0 ± 5.1	130.6 ± 6.6	111.5 ± 3.5
	$\log(Z_{Q,G}$ (μW g^{-1}))	20.84 ± 0.87	–	20.84 ± 0.77	20.81 ± 0.90	21.02 ± 0.76	20.20 ± 0.98	17.58 ± 0.51
	Correlation coefficient	0.9991	–	0.9993	0.9990	0.9993	0.9987	0.9995
					Pairs of temperatures evaluation			
89–80	$Ea_{Q,G}$ (kJ mol^{-1})	146.2	–	145.3	145.9	144.9	143.3	118.1
	$\log(Z_{Q,G}$ (μW g^{-1}))	22.49	–	22.29	22.52	22.45	22.05	18.55
80–70	$Ea_{Q,G}$ (kJ mol^{-1})	125.7	–	127.3	124.7	127.0	120.3	106.1
	$\log(Z_{Q,G}$ (μW g^{-1}))	19.46	–	19.62	19.39	19.81	18.65	16.77

A calculation of the parameters using pairs of temperatures is shown, indicating the tendency of the change in the parameters going from higher to lower temperatures. The change in activation energy with temperature is greater than the standard deviations.

formulation. The permitted limit value Q_L is typically 97% of the reference, means a reduction in energy or an energy loss of 3%. For the standard case, the times $ty_{Q,L}(T)$ must be determined using Eq. (10) [9].

$$y_{Q,L} = \frac{Q_L}{Q_{reference}} = 1 - \frac{Q(ty_{Q,L}(T))}{Q_{reference}} \quad (9)$$

$$(1 - y_{Q,L})Q_{reference} = \int_0^{ty_{Q,L}(T)} \frac{dQ(t,T)}{dt}\,dt \quad (10)$$

For a zero order reaction Eq. (10) simplifies to Eq. (11). According to Eq. (12) the needed HGR values can be calculated at the required temperatures with the Arrhenius parameters. Tables 9 and 10 shows the times necessary to reach an energy loss of 3% at 50 °C, using the Arrhenius parameters determined between 70 and 89 °C.

$$ty_{Q,L}(T) = \frac{(1 - y_{Q,L})Q_{reference}}{dQ(T)/dt} \quad (11)$$

$$\ln\left(\frac{dQ(T)}{dt}\right) = \ln(k_{Q,G}(T)) = \ln(Z_{Q,G}) - \frac{Ea_{Q,G}}{RT} \quad (12)$$

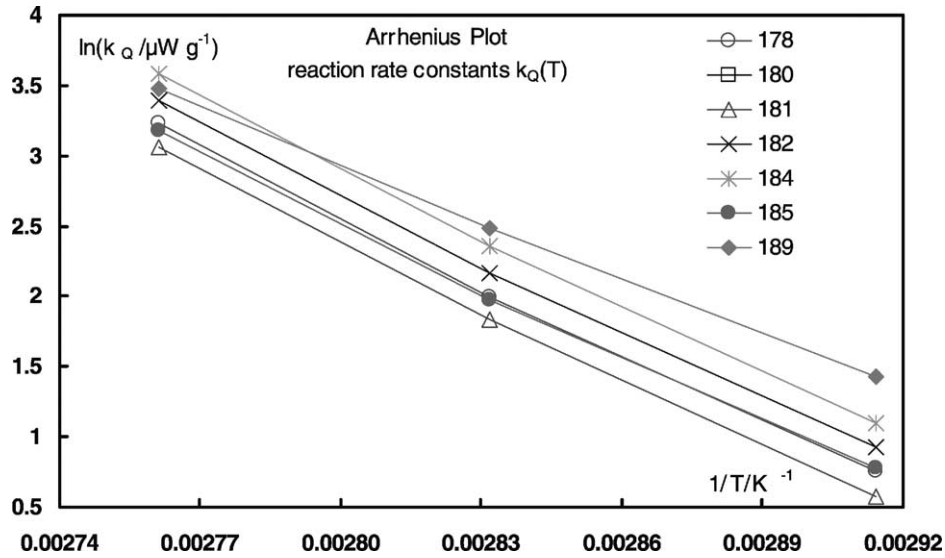

Fig. 9. Arrhenius plot of the reaction rate constants $k_Q(T)$ from heat generation rate measurements. The tendency of decreasing activation energy with decreasing temperature is indicated. The reversal in the reactivity order between HFK 189 and 184 can be seen. HFK 180 was not measured.

Table 9
Factors for increase/decrease of the reaction rate constant in heat generation rate with a 10 °C temperature step, determined according to the experimental data and calculated with the derived activation energies (from 70 to 89 °C)

Temperature range (°C)	178		180		181		182		184		185		189	
	Experimental	Ea	Experimental	Ea	Experimental	Ea	Experimental	Ea	Experimental	Ea	Experimental	Ea	Experimental	Ea
90–100		3.31	–	–		3.32		3.29		3.31		3.19		2.69
80–90	3.94	3.54	–	–	3.91	3.56	3.93	3.52	3.89	3.55	3.83	3.40	3.03	2.84
70–80	3.48	3.81	–	–	3.54	3.83	3.45	3.79	3.53	3.82	3.30	3.65	2.87	3.02
60–70		4.13	–	–		4.15		4.10		4.14		3.95		3.23

The factors for the step 80–90 °C was calculated using the extrapolated heat generation rate values (see Table 3).

Table 10
Times $ty_{Q,L}$ in years to reach 3% energy loss at 50 °C calculated using Eq. (11)

	178	180	181	182	184	185	189
$Q_{EX,gw}$ (J g^{-1})	4540	4670	4700	5050	4880	4510	4750
$ty_{Q,L}$ (50 °C)/*a*	38.4	–	49.7	36.6	29.4	34.9	12.5
$r_{C,FK}$ (50 °C)/*m*	3.78	–	4.22	3.51	3.19	3.68	2.32
$r_{C,FK}$ (71 °C)/*m*	0.87	–	0.97	0.81	0.73	0.89	0.70
$r_{C,FK}$ (90 °C)/*m*	0.27	–	0.30	0.25	0.23	0.28	0.27
$r_{C,FK}$ (110 °C)/*m*	0.09	–	0.10	0.08	0.07	0.10	0.11

The reference quantity $Q_{reference}$ is the heat of explosion with gaseous water $Q_{EX,gw}$. Furthermore the critical radius $r_{C,FK}$ (values in meters) is listed according to Frank–Kamenetzkii for a cylindrical shape (infinite length) at several environmental temperatures Tw between 50 and 110 °C, calculated using Eq. (13).

Table 10 also contains additional data for the thermal critical radius of the HFK batches, calculated according to the Frank–Kamenetzkii description of thermal explosion caused by self heating in stationary phases, Eq. (13). The meaning of the symbols is given with the equation. The value of the dimensionless critical Frank–Kamenetzkii parameter δc is 2.0 for a cylinder with infinite length. The values of 0.2 W m^{-1} K^{-1} and 1.6 g cm^{-3} have been taken for heat conductivity and mass density. Based on the Arrhenius parameters of Table 8 between 70 and 89 °C, the results for the values of $r_{C,FK}$ show that problems may arise if heating of the propellant cannot be avoided when the rocket system is at high speed.

$$r_{C,FK} = \sqrt{\frac{\delta c \lambda}{\rho} \frac{RTw^2}{Ea_{Q,G}} \frac{1}{Z_{Q,G}} \exp\left(+\frac{Ea_{Q,G}}{RTw}\right)} \qquad (13)$$

where δc is the critical Frank–Kamenetzkii parameter (FKP_C), its value is shape dependent; $r_{C,FK}$ the thermal critical radius at given wall temperature Tw; ρ the mass density; λ the heat conductivity; Tw the storage temperature (wall temperature of the sample) in Kelvin; R the general gas constant; $Ea_{Q,G}$ the activation energy of the global heat generation rate; and $Z_{Q,G}$ is the pre-exponential factor of the global heat generation rate.

4. Conclusion

The ranking of the HFK batches corresponding to their ageing rate is: according to mass loss, evaluated with k_{ML}

90 °C	184 > 189 > 182 > 185 > 178 > 180 ≈ 181
80 °C	189 > 184 > 182 ≈ 185 > 178 > 181 ≈ 180
70 °C	189 ≫ 184 > 185 ≈ 182 > 178 > 181 > 180

according to heat generation rate, evaluated with HGR in the linear region

89 °C	184 > 189 > 182 > 178 > 185 > 181 (no data for 180)
80 °C	189 > 184 > 182 > 180 > 178 > 185 > 181
70 °C	189 ≫ 184 > 182 > 185 ≈ 178 > 181 (no data for 180)

The main sequence is determined by the nitric acid esters BTTN and TMETN which explains the series of 189, 184 and 182. After the position of HFK 182 the differences in the rates are quite small, and the more detailed ranking following the position of HFK 182 seems to be co-influenced by the reactive interaction between GAP and ε-CL20 [10]. A different temperature dependence is indicated for HFK 189. It shows a lower activation energy than the other batches. However, based on the summarised chemical decomposition reactions, the thermal ageing behaviour of all investigated HFK batches is favourable, in spite of the lack of stabilisers for the nitric acid ester plasticizers. Both measurement methods mass loss and heat generation rate provide congruent information on the ageing of the HFK batches.

Acknowledgements

Dr. Klaus Menke and Mr. Siegfried Eisele, both at ICT, have designed and manufactured the HFK

batches. The work was financed by the German Bundesministerium für Verteidigung (BMVg).

References

[1] S. Eisele, K. Menke, About the burning behaviour of smoke reduced composite propellants based on AP/CL20/GAP, in: Proceedings of 32nd International Annual Conference of ICT, pp. 149.1–149.18, 3–6 July 2001, Karlsruhe, Germany, Fraunhofer-Institut für Chemische Technologie (ICT), Postfach 1240, D-76318 Pfinztal-Berghausen, Germany.

[2] STANAG (Standardization Agreement) 2895, Extreme climatic conditions and derived conditions for use in defining design and test criteria for NATO forces material, NATO Headquarters, Military Agency for Standardization, Bruxelles, Belgium, 1990.

[3] H. Bathelt, F. Volk, M. Weindel, The ICT thermochemical data base, in: Proceedings of 30th International Annual Conference of ICT, pp. 56.1–56.12, 29 June–2 July 1999, Karlsruhe, Germany, Fraunhofer-Institut für Chemische Technologie (ICT), Postfach 1240, D-76318 Pfinztal-Berghausen, Germany.

[4] R. Meyer, J. Köhler, A. Homburg, Explosives, 5th ed., Wiley-VCH Verlag GmbH, Weinheim, Germany, 2002.

[5] Encyclopedia of explosives and related items, in: B.T. Fedoroff, S.M. Kaye (Eds.), Picatinny Arsenal, Dover, New Jersey, USA, 1960–1983, vol. 1: Ignition test (Deflagration Test), Vacuum Stability Test, pp. VII–XXVI, vol. 5: Dutch Stability Test, p. D1580, vol. 10: Vacuum Stability Test, p. V1.

[6] Vacuum Stability Test, MIL-STD 286B, Method 403.1.2.

[7] M.A. Bohn, Modelling of the stability, ageing and thermal decomposition of energetic components and formulations using mass loss and heat generation, in: Proceedings of the 27th International Pyrotechnics Seminar, Grand Junction, Colorado, USA, 16–21 July 2000, pp. 751–770.

[8] M.A. Bohn, Kinetic description of mass loss data for the assessment of stability, compatibility and aging of energetic components and formulations exemplified with ε-CL20, Propel. Explosives Pyrotech. 27 (2002) 125–135.

[9] M.A. Bohn, Kinetic description of the ageing of gun and rocket propellants for the prediction of their service lifetime, in: T. Trevor (Ed.), Proceedings of the 1st Workshop on the Microcalorimetry of Energetic Materials, 7–9 April 1997, Leeds, UK, Griffiths, QinetiQ (former DERA), Fort Halstead, Sevenoaks, Kent TN14 7BP, UK.

[10] V. Thome, P.B. Kempa, M.A. Bohn, Erkennen von Wechselwirkungen der Nitramine β-HMX und ε-CL20 mit Formulierungskomponenten durch Computersimulation, in: Proceedings of 31st International Annual Conference of ICT, Karlsruhe, Germany. Fraunhofer-Institut für Chemische Technologie (ICT), Postfach 1240, D-76318 Pfinztal-Berghausen, Germany, 27–30 June 2000, pages 63.1–63.20.